Shear behavior of steel I-girder with stiffened corrugated web, Part II Numerical study

He, Jun; Wang, Sihao; Liu, Yuqing; Wang, Dalei; Xin, Haohui

DOI
10.1016/j.tws.2019.02.023

Publication date
2020

Document Version
Final published version

Published in
Thin-Walled Structures

Thin-Walled Structures 147 (2020) 106025

Contents lists available at ScienceDirect

Thin-Walled Structures

journal homepage: www.elsevier.com/locate/tws

Full length article

Shear behavior of steel I-girder with stiffened corrugated web, Part II: Numerical study

Jun He[a], Sihao Wang[b], Yuqing Liu[b,*], Dalei Wang[b,*], Haohui Xin[c]

[a] School of Civil Engineering, Changsha University of Science and Technology, Hunan, China
[b] Department of Bridge Engineering, Tongji University, Shanghai, China
[c] Civil Engineering and Geosciences, Delft University and Technology, Netherlands

ARTICLE INFO

Keywords:
Composite bridge
Stiffened corrugated steel web
Finite element analysis
Parametric studies
Shear capacity
Analytical models evaluation

ABSTRACT

For long-span composite bridges with corrugated steel webs, the encased concrete near the intermediate support section increases the weight of the girder, reduces pre-stressing efficiency, and causes difficulties in the construction process. The authors in the companion paper [1] proposed a corrugated steel web with vertical or/and horizontal stiffeners to replace or shorten the length of concrete encasement. In parallel with experimental study described in the companion paper, this paper further investigates the shear performance of proposed stiffened corrugated steel webs by numerical and analytical methods. Firstly, finite element (FE) models considering material nonlinearity, welding residual stress, and geometric imperfection were established and validated against the experimental results. Then the effects of web thickness, corrugation depth, height and thickness of stiffeners on shear strength and failure modes were analyzed based on the validated FE models. Finally, both experimental and numerical shear strength were used to evaluate the applicability of existing calculation methods proposed by different scholars to predict the shear capacity of stiffened corrugated steel web. The comparisons reveal that calculation methods proposed by Hassanein & Kharoob [2] and Leblouba et al. [3] predict the shear capacity of pure corrugated steel web more accurately, and all existing calculation methods underestimate corrugated steel web with vertical stiffeners. Therefore, the analytical model for accurately predicting shear strength of stiffened corrugated steel web need to be developed, which will be investigated in subsequent studies.

1. Introduction

Steel-concrete composite bridge with corrugated steel web represents a promising structural system, which has been widely built around the world in the past three decades. This type of bridge uses corrugated steel webs to substitute conventional concrete webs in I-girder or box-girder, which reduces the self-weight of the bridge girder, prevents cracking of the web, improves prestressing application efficiency, and makes full use of the benefits of combining two construction materials [4,5]. Most of composite bridges with corrugated steel webs are continuous girder bridges and rigid frame bridges with medium or large spans, the concrete encasement (Fig. 1a) is generally arranged to enhance the stability of corrugated steel webs near the intermediate supports where subjected to large shear force and hogging moment, which has been proved to be effective [6,7]. But the encased concrete also bring some problems, such as increases the complexity of construction process, increases the weight of composite girder near the support section, limits the accordion effect in longitudinal direction, reduces the prestressing efficiency at intermediate support area, and causes stress concentration at the transition section between pure corrugated steel web and encased composite web [8,9].

In order to overcome these shortcomings, corrugated steel web with vertical and horizontal stiffeners was proposed to replace concrete encasement (Fig. 1b) or as a transition between pure corrugated web and encased composite web (Fig. 1c) to shorten the length of encased concrete. The vertical stiffeners are welded on each parallel and inclined fold of corrugated steel web, and trapezoid-shaped horizontal stiffeners are welded between two adjacent inclined folds on both sides of the web. The general profile and geometric notations of stiffened corrugated steel web are shown in Fig. 2, in which, a is the parallel fold width; b is the horizontal projection of the inclined fold width; c is the inclined fold width; d is the corrugation depth; α is the corrugation angle; t_w and t_s are the thickness of corrugated web and stiffeners respectively; h_s is the width of the stiffeners. The stiffened corrugated

* Corresponding authors.
E-mail addresses: yql@tongji.edu.cn (Y. Liu), wangdalei@tongji.edu.cn (D. Wang).

https://doi.org/10.1016/j.tws.2019.02.023
Received 31 August 2018; Received in revised form 21 December 2018; Accepted 15 February 2019
Available online 27 March 2019

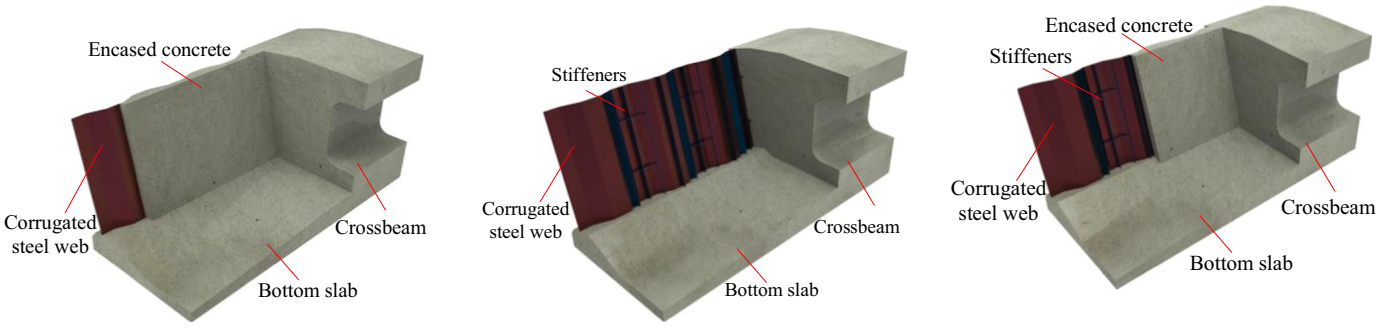

(a) Web with encased concrete (b) Web with stiffeners (c) Web with a combination of encased concrete and stiffeners

Fig. 1. Web configuration near intermediate supports.

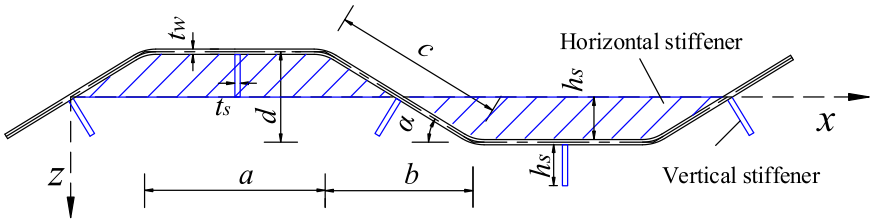

Fig. 2. Profile and geometric parameters of corrugated steel web.

steel webs are directly welded and fabricated in a factory, thus avoiding complex in-situ concrete casting. In addition, stiffeners are expected to improve shear buckling strength of the corrugated steel web during construction process and at service stage. Therefore, stiffened corrugated steel web can be utilized in the intermediate support area of the composite bridge, and its shear behavior also needs to be paid special attention to.

For corrugated steel plates, the progress of experimental study on shear behavior has been presented in the companion paper [1], this paper focuses on the analytical and numerical investigations: Easley et al. [10,11] proposed the global shear buckling equation of corrugated steel web under different boundary conditions by treating the corrugated steel web as an orthotropic flat web. The corrugated steel web is assumed to provide the shear capacity of the girder, while the shear strength is controlled by buckling and/or shear yielding of the web. Elgaaly et al. [12] performed a nonlinear analysis using the program ABAQUS, and the initial imperfections were first introduced into the finite element model to simulate the test results. Moreover, the ultimate shear capacity calculation methods based on global and local buckling modes were presented. Luo and Edlund [13] conducted numerical studies on the shear capacity of corrugated web using nonlinear finite element method, the influence of parameters such as the web thickness, corrugation depth, corrugation angle, and fold width on shear capacity and buckling modes were reported, empirical formulas for predicting shear strength were examined, and design suggestions for such girders in shear were given. Yi et al. [14] studied the nature of interactive shear buckling of corrugated webs by finite element analysis, and concluded that the first order interactive shear buckling equation not considering material inelasticity and material yielding provides a good estimation of the shear strength of corrugated steel web by comparison with experimental and finite element analysis (FEA) results. Eldib [15] carried out FEA to investigate the geometric parameters affecting the shear strength of curved corrugated steel web. Compared with trapezoidal corrugated steel web with the same web thickness, the curved corrugated steel has higher shear strength. The design criteria of curved corrugated steel web were proposed and validated by an experimental data in the literature. Sause and Braxtan [16] summarized previously developed formulas for predicting the shear strength of the corrugated steel web and proposed a new formula along with corresponding theory. Hassanein and Kharoob [2,17] found that when the ratio of flange's thickness to corrugated steel web's thickness was greater than 3, the boundary conditions between flange and web were approximately fixed, and the formula for calculating the interactive shear buckling of corrugated webs under fixed boundary conditions was proposed. On the basis of finite element parametrical analyses considering geometric and material nonlinearity, it was concluded that the formula of interactive shear buckling strength proposed by Hassanein & Kharoob [2] and the formula of shear loading capacity proposed by Sause & Braxtan [16] have high accuracy.

At present, there are few reports about shear behaviors of corrugated steel web with vertical or/and horizontal stiffeners. Wang et al. [1] tested four corrugated steel web I-girders with different arrangements of stiffeners to investigate their shear performance. The experimental buckling modes, shear capacity, stress distributions of corrugated steel web and welded stiffeners were observed and analyzed in detail. The present paper pays more attention to the numerical studies of stiffened corrugated steel web girders. Firstly, finite element models considering material nonlinearity, residual stress, and geometric nonlinearity are established and validated by model test results. Then parametric analyses are performed to examine the effects of web thickness, corrugation depth, height and thickness of stiffeners on the shear behavior. Finally, the applicability of existing methods for calculating the shear capacity of corrugated steel webs to that of stiffened corrugated steel webs is evaluated through the comparisons of experimental and numerical results.

2. Finite element modeling

2.1. Description of test specimens

Four steel I-girders with pure or stiffened corrugated web designated as W1~W4 were fabricated and tested to investigate their shear performance in the companion paper [1].

The dimensions and configurations of test specimens are shown in Fig. 3. The difference between each specimen is the stiffeners' arrangement. The total length and height of test specimens are 4.4 m and

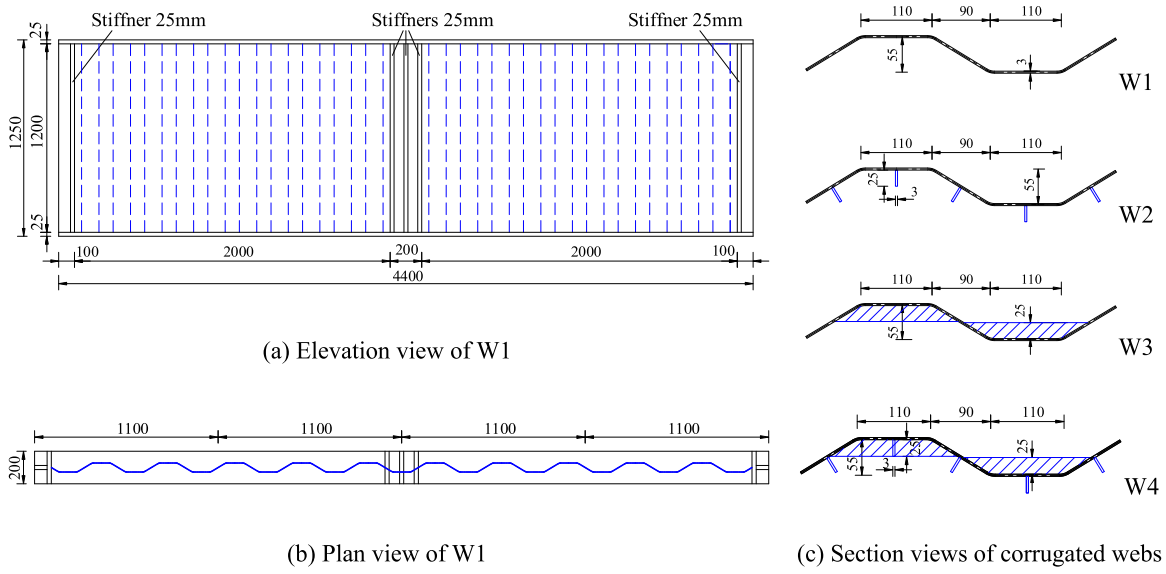

Fig. 3. Test specimens (mm).

1.25 m, respectively. The unit wavelength of corrugated web is 400 mm, the width of parallel fold (a), inclined fold (c), and the projected width of inclined fold (b) is 110 mm, 105.5 mm, and 90 mm, respectively. The corrugation depth (d) and angle (α) are 55 mm and 30°, respectively. The thickness of corrugated steel web (t_w), horizontal and vertical stiffeners (t_s) is 3 mm; while the thickness of top and bottom steel flanges (t_f) is 25 mm. The height of horizontal and vertical stiffeners (h_s) is 25 mm. The vertical stiffeners were welded in the middle of each fold, while the horizontal stiffeners were welded at a distance of 270 mm from the top flange.

2.2. Finite element model

The nonlinear finite element analysis (FEA) program ANSYS (version 16.0) was used to model the shear behavior of steel I-girders with stiffened corrugated web, considering the effect of initial geometric imperfections, welding residual stress, and material nonlinearity. Two analysis types were adopted: the elastic bifurcation analysis was performed on a perfect corrugated web to obtain the first buckling mode shape, and then a nonlinear buckling analysis was used to investigate the ultimate shear strength of stiffened corrugated web girders. The corrugated steel webs, steel flanges, and welded stiffeners were simulated by a 4-node structural shell element SHELL181 based on the mesh sensitive analysis in Section 2.3. Each node has six degrees of freedom, namely three translations in the nodal x, y, and z directions, respectively, and three rotations about the nodal x-, y-, and z-axes, respectively. The element has plasticity, stress hardening, large deflection, and large strain capabilities.

Fig. 4 shows the finite element model, boundary condition and loading of specimen W2. The boundary conditions were simulated the same as that in shearing tests: the test specimens were simply supported, all translational degrees of freedom and rotational degrees of freedom were restrained at side A to simulate fixed bearing. The translational degree of freedom (with respect to Y-axis) and rotational degrees of freedom (with respect to X-, Y-axis) were restrained at side B to simulate roll bearing. The translational degree of freedom (with respect to Z-axis) at two support ends (lines AD and BC), top and bottom flanges in mid-span (area E and F) were restrained to simulate lateral supports and lateral displacement limit device. The test specimens were subjected to concentrated load on the top flange, the force control method and appropriate load steps were chosen during the loading process to improve the accuracy and convergence of simulation results. Full Newton-Raphson iterative procedure was used to solve the nonlinearity by continuously updating the element stiffness matrix.

2.3. Mesh sensitivity analysis

Previous researches [15,18,19] show that mesh sensitivity has a great influence on the shear strength of corrugated steel web, and the number of elements per sub-panel of the corrugation should be properly adopted. Therefore, mesh sensitivity analysis was carried out to assess the requirement of the mesh refinement as well as the applicable element type in numerical modeling. Fig. 5 shows the results of mesh sensitivity analysis for specimen W1 without stiffeners and specimen W2 with vertical stiffeners. The finite element analysis results converge on a stable value when the number of elements per sub-panel is larger

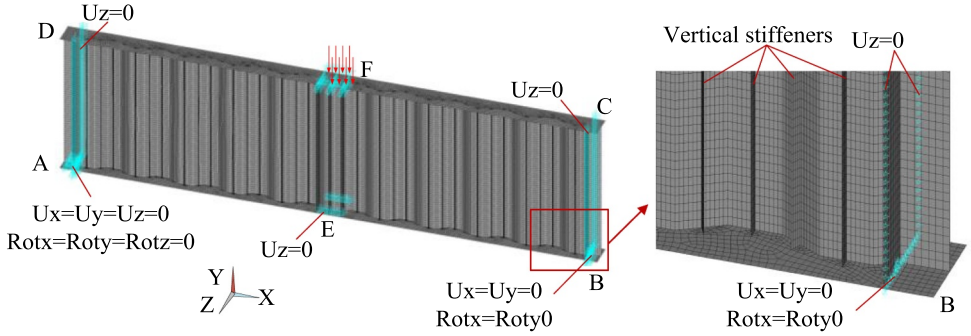

Fig. 4. Finite element model of specimen W2.

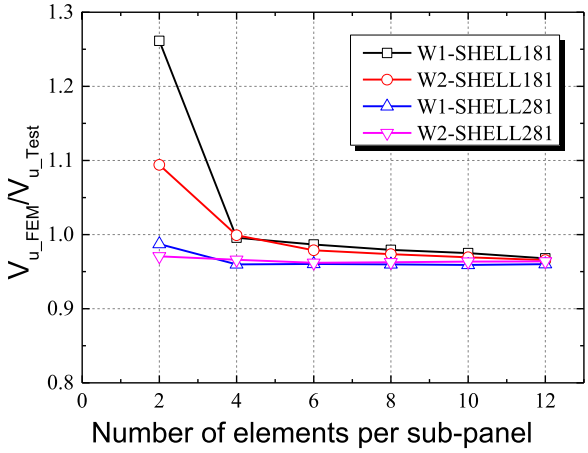

Fig. 5. Results of mesh sensitivity analysis.

than 4 in the case of eight-node-shell elements (SHELL281). For corrugated steel web modeled by four node-shell elements (SHELL181), the analysis loading capacity decreased with the increase of the divided element number per sub-pane and converged to the same value as eight-node-shell elements (SHELL281) when the sub-panel is divided into 12 elements. Considering the introduction of welding residual stress in finite element model, the more elements divided per sub-panel, the more accurate the residual stress can be introduced into the model. Therefore, 12 elements along the width of the web folds using four node-shell elements (SHELL181) were adopted to get accurate analytical results and minimize the computational effort.

2.4. Material constitutive sensitivity analysis

2.4.1. Material constitutive of corrugated steel web

The corrugated steel webs are cold-formed thin-walled members, and plastic deformation is inevitable to occur due to cold forming process, which cannot be completely released after cold bending, resulting in significant change in material properties [20]. According to related study by Abdel-Rahman & Sivakumaran [21], the strength of steel plate was greatly improved after cold bending, and its yield strength (strength corresponding to 0.2% plastic strain) and ultimate strength were increased by 23–47%. The increase of strength is accompanied by deterioration of the ductility of steel plate. The stress-strain curves of cold-formed steel do not appear the yield plateau and the strength-harden section like ordinary steel plates do, which generally exhibit an initial linear variation and then gradually increase to ultimate strength. Abdel-Rahman & Sivakumaran [21] and Karren [22] proposed calculation formula of the yield strength of steel plate after cold bending and provided a corresponding constitutive model, but their research objects were tubular or trough sections, the applicability of this constitutive model in trapezoid corrugated steel web of bridge structure needs to be further explored.

Since corrugated steel web is formed by cold bending, the relationship between the stress and strain of corrugated steel web is different from that of flat steel plate. In the shear loading test, the corrugated web presented interactive buckling and shear yielding, which also occurred for specimens with stiffeners. Therefore, material constitutive sensitivity analyses need to be performed to obtain proper stress-strain relationship. Four different constitutive models were adopted, including elastic-perfect plastic model (EPP) [13], elastic-plastic hardening model considering yield plateau (EPYP) [23], elastic-linear strength hardening model (EPSH) [24] and Ramberg-Osgood model (RO) considering the strength-hardening section [25], as shown in Fig. 6. For steel girders with corrugated steel web under path loading, Luo & Edlund [25] found that the loading capacity obtained by Ramberg-Osgood model can be increased by 8~12% in comparison with that by ideal elastoplastic model. The stress-strain relationship of Ramberg-Osgood model is expressed as follows:

$$\varepsilon = \frac{\sigma}{E} + \frac{p}{100}\left(\frac{\sigma}{\sigma_p}\right)^n \tag{1}$$

where σ and ε are the stress and strain, respectively, and σ_p is the stress corresponding to residual plastic strain at p%, and for low carbon steel, $p = 0.2$. The parameter n is the enhancement coefficient of stress-strain curve, for corrugated steel plate, $n = 8$ [25]. For the stiffeners and top/bottom steel flanges, the elastic-plastic hardening model considering yield plateau was adopted. All constitutive models use Von Mises yield criterion, which is applicable to proportional loading and large plastic strain of steel. The Young's modulus E and Poisson's ratio μ are taken as 203 GPa and 0.3 respectively, the yield strength f_y and ultimate strength f_u of corrugated steel web were adopted as 400 MPa and 524 MPa respectively according to material tests.

2.4.2. Effect of material constitutive

Fig. 7 shows the effect of different constitutive models on load-deflection curves and loading capacity. It can be found that different constitutive models do not affect the initial stiffness of test specimens, and the load-deflection curve from RO model exhibits nonlinearity behavior earlier than those from other three models. The loading capacity from EPP and EPYP models are almost the same, while the loading capacity from EPSH model is slightly larger than that from EPP and EPYP models. For specimens W1 and W3 with elastic buckling failure, the simulated loading capacity from RO model is less than those from other three models. For specimens W2 and W4 with vertical stiffeners, the loading capacity from RO model is larger than those from other three models, and the relative error between different constitutive models for the same specimen is within 10%. In all, the RO model coincides well with the test results, which was adopted in the following finite element analysis.

2.5. Residual stress sensitivity analysis

2.5.1. Residual stress distribution

Residual stress plays an important role in the design of steel members, which seriously affects the mechanical properties of the material. There are many factors causing residual stress, such as welding, cold bending, hot rolling, flame-cutting, punching and so on [26]. For steel beams with stiffened corrugated web, there are three factors may induce residual stress in corrugated webs [27]: (a) the cooling of weld metal between corrugated steel web and steel flanges; (b) bending regions of corrugation due to cold forming; (c) the cooling of weld metal between corrugated steel web and stiffeners. The oxygen cutting and cooling of weld metal also produce residual stress in steel flanges, the stress distribution pattern and its influence on flange buckling behavior have been measured and studied by Li et al. [28] and Jáger et al. [29]. The residual stress in the flanges was not considered in the following analysis because the buckling failure was only occurred in the corrugated steel web.

The residual stress distribution on corrugated steel web has been investigated by some researchers. Fig. 8a shows the schematic drawing of residual stress distribution adopted by Sumiya et al. [30], the edge of corrugated web welded with flanges is tension yielded, and reduced linearly along the web height to uniformly distributed compressive strength of $0.1f_y$. Koichi and Masahiro [31] proposed the similar residual stress distribution of corrugated steel web, but the compressive strength along the web height was taken as $0.3f_y$, which has also been adopted by Jáger et al. [23]. The thickness and height of corrugated web in the shear test of Sumiya et al. [30] were 3.2 mm and 1200 mm, while the height of corrugated webs in Koichi and Masahiro [31] test was just 320 mm, which may be the reason for different residual compressive stress distributions. In the following finite element

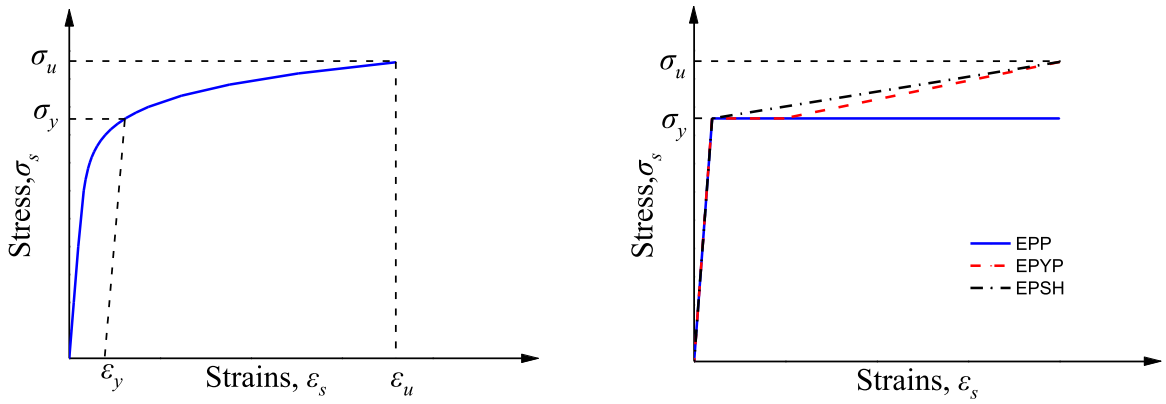

(a) Corrugated steel web (b) Flanges and stiffeners

Fig. 6. Constitutive model of stress-strain relationship.

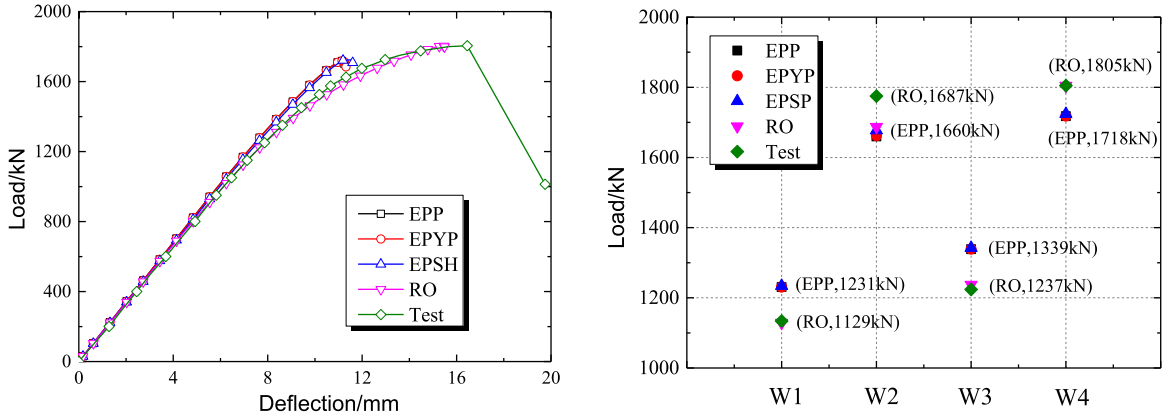

(a) Load-deflection curves for specimen W4 (b) Ultimate loads from different constitutive models

Fig. 7. Results of material constitutive sensitivity analysis.

analysis, the residual stress distribution proposed by Sumiya et al. [30] was adopted because of the similar dimensions of test specimens.

When the vertical and horizontal stiffeners are welded to corrugated steel webs, the welding residual stress is generated in the web and stiffeners after welds cooling, which also affects the shear strength of stiffened corrugated steel webs. Welding residual stresses of stiffened plates commonly used in bridge structures have been extensively studied, and different models of welding residual stress distribution have been proposed. Fig. 8b–c show the simplified model of welding residual stress adopted by Gannon et al. [32], which assumes that a certain range near the weld of mother plate is tension yielded, and the rest is a uniformly distributed residual compressive stress. In Fig. 8b, b_t is the width of tension area for mother plate, and t is the thickness of mother plate, η is the width coefficient of tension area. Faulkner [33] suggested that the value of η is generally between 3 and 4.5, η is taken as 3 in this study. The residual compressive stress f_r is generally 0.25–0.3 times of the yield stress f_y of mother plate [34–36], f_r is taken as $0.25f_y$. For the stiffeners, the residual stress is reduced linearly along stiffener height from the tensile yield strength f_y at welding to the compressive strength of $1/4f_y$ at one-quarter of stiffener height ($h_s/4$), then linearly reduced to zero from $h_s/4$ to h_s, where h_s is the height of stiffener.

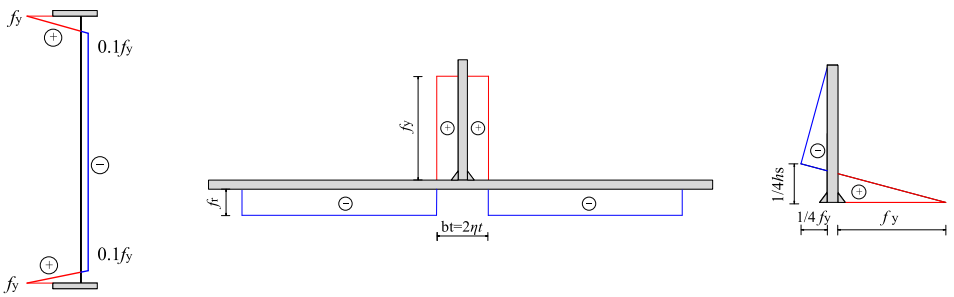

(a) Corrugated web (b) Sub-panel of the corrugated web (c) Stiffeners

Fig. 8. Residual stress distribution of stiffened corrugated steel webs.

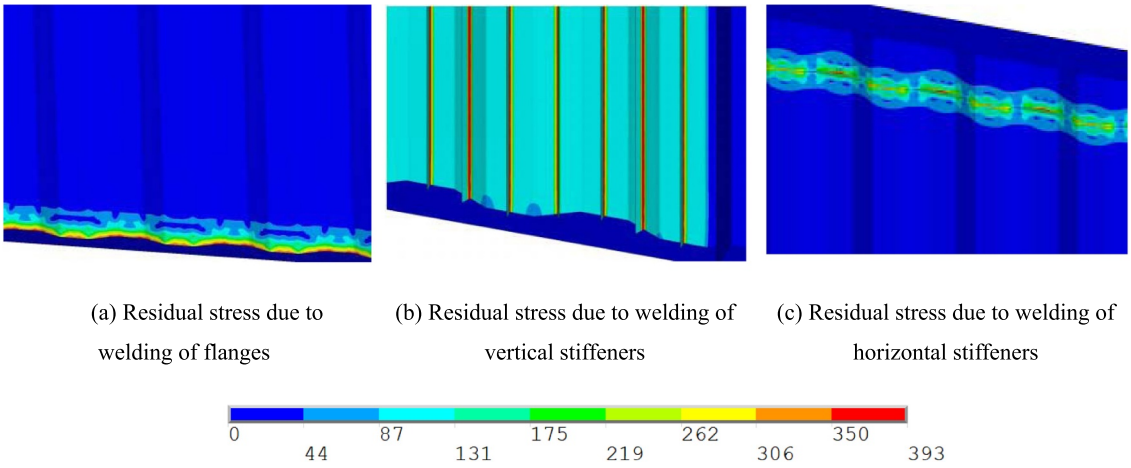

(a) Residual stress due to welding of flanges (b) Residual stress due to welding of vertical stiffeners (c) Residual stress due to welding of horizontal stiffeners

Fig. 9. Welding residual stress distribution in the finite element model (MPa).

2.5.2. Effect of residual stress

In order to investigate the effect of residual stress on shear capacity of stiffened corrugated steel web, the finite element models with or without consideration of residual stress (W-R, W/O-R) of test specimens were established to conduct the nonlinear analysis. Fig. 9 presents the defined residual stress distribution due to welding of flanges, vertical and horizontal stiffeners in the FE models.

Fig. 10a shows the effect of residual stress on load-deflection curves and loading capacity. The residual stress does not affect the initial stiffness of each specimen, but leads to load-deflection curves entering into nonlinearity in advance for specimens with vertical stiffeners. In addition, the residual stress reduced the loading capacity of corrugated steel web girders, the corresponding reductions for specimens W1~W4 are 6.1%, 7.3%, 2.4% and 3.5%, respectively. The reduction of loading capacity for specimen W3 was smaller than that for specimen W1, the welding of lateral stiffeners reduced the effective height of corrugated web, which also decreased the sensitivity of loading capacity to residual stress. The effect on loading capacity of residual stress induced by horizontal stiffeners can be negligible, since the welding residual stress is only distributed near the horizontal stiffeners. For specimen W2, the reduction of loading capacity is the largest by combining the residual stress caused by welding of vertical stiffeners and steel flanges at the same time.

2.6. Equivalent geometric imperfections sensitivity analysis

2.6.1. Geometric imperfections distribution

In the process of cold bending, welding, and assembling, the initial geometric imperfections are unavoidable to appear, which seriously affect the shear strength of the corrugated steel web, Elgaaly et al. [12] found that the shear capacity obtained from finite element analysis was higher than that from tests. After introducing imperfections in the form of a global double sine wave, better agreement between the analytical and experimental results was obtained. Abbas et al. [37] analyzed the influence of geometrical imperfection (including imperfection shape and amplitude) of the corrugated steel web on shear strength by nonlinear finite element method. The results showed that shear capacity decreased with the increasing of the imperfection amplitude, and the first mode provided the most critical condition. Driver et al. [38] measured the initial imperfections of corrugated steel web for shear test specimen by hand and electrical measurements. The results indicated that the initial imperfection shape showed sinusoidal distribution along the web height, the maximum imperfection amplitude was 6 mm, which was equal to the thickness of the corrugated steel web (t_w). Therefore, they suggested imperfection amplitudes of t_w should be considered in finite element simulations.

2.6.2. Equivalent geometric imperfections

EN1993-1-5 [39] states that the initial imperfections include geometric imperfections and residual stresses, which can be considered

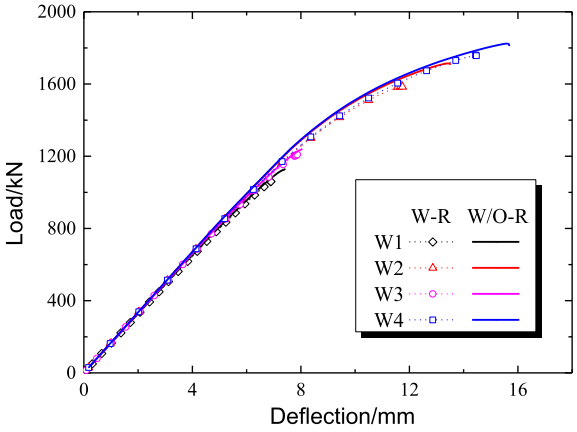

(a) Load-deformation curves

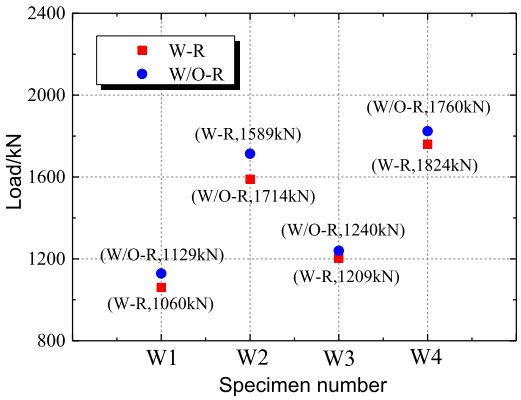

(b) Relationship between loading capacity and residual stress

Fig. 10. Effect of welding residual stress.

simultaneously by equivalent geometric imperfections in the finite element model. The model should include imperfections corresponding to the most likely instability modes, usually, the application of the first order buckling mode scaled to proposed amplitude is the best choice, and the calculated results tend to be relatively conservative [40], which was adopted in the following FE model validation and numerical parametric studies.

The amplitude of equivalent geometric imperfection should be properly considered. EN1993-1-5 [39] recommends taking $h_w/200$ (h_w is the web height) for flat web girders, which was confirmed to be applicable for corrugated web girders by Yi et al. [41] and Jáger et al. [40]. Driver et al. [38] suggested that the imperfection amplitude was equal to the web thickness t_w, which was also accepted by Leblouba et al. [42], Hassanein and Kharoob [17]. At present, there is no definite method to obtain the geometric amplitude, and large differences exist in various methods. In addition, the imperfection in different direction causes different amount of deformation. Thus, it is necessary to check different directions of imperfections for unsymmetrical plates like specimen W2 and W4 with vertical stiffeners.

2.6.3. Effect of equivalent geometric imperfections

In order to perform an adequate numerical parametric study, a sensitivity analysis is executed for the determination of equivalent geometric imperfection amplitude. The elastic buckling analysis was first carried out before nonlinear finite element analysis to obtain the first order buckling mode each specimen, and then the first order buckling mode with different scaling factor range from −10 to 10 mm at an increment of 2 mm was introduced into finite element model as equivalent geometric imperfection.

Fig. 11a shows the effect of imperfection amplitude on the load-deflection curve and loading capacity for each specimen. The imperfection amplitude does not affect the initial stiffness of stiffened corrugated steel web girder, but increasing the imperfection amplitude leads to a significant reduction in loading capacity of each specimen. When the imperfection amplitude (I/A) increased from 0 to 2 mm, the loading capacity of specimens W1∼W4 decreased by 19.6%, 15.6%, 17.6%, and 12.1%, respectively. Afterward, the loading capacity decreased approximate linearly with the increase of imperfection amplitude, and the reduction of loading capacity for specimens W1∼W4 are 14.7%, 10.3%, 12.5%, and 8.2% respectively when the positive imperfection amplitude increased by 2 mm. Compared to specimen W1 with pure corrugated web, the reduction degree of stiffened corrugated web is relatively smaller, indicating that the sensitivity of corrugated steel webs to geometric imperfection decreased after the welding of stiffeners. In addition, the application of horizontal stiffeners combined with verticals shows less sensitivity than the application of horizontal or vertical stiffeners separately. With the increasing of the negative imperfection magnitudes, the reduction of loading capacity for specimens W1∼W4 are 14.6%, 11.1%, 12.8%, and 9.1% respectively. Therefore, the positive imperfection shape tends to be worse than the negative imperfection shape for specimen W2 and W4 with unsymmetrical stiffeners.

From the geometric imperfections sensitive analysis, it can be concluded that the loading capacity was sensitive to the geometric imperfections amplitude. In order to get the calculation results consistent with the test ones, the equivalent imperfection amplitude should be taken as 6 mm (1/200 of the web height h_w) for specimens W1 and W3 without vertical stiffeners. For specimen W2 and W4, the equivalent imperfection amplitude is smaller than that for W1 and W3, due to the welding of vertical stiffeners, and 3 mm (equal to the web thickness t_w) was adopted as equivalent imperfection amplitude in the following FE model validation and parametrical analysis.

3. FE model validation

3.1. Failure modes

Fig. 12 shows the comparison of failure mode between test results and FEA ones by introducing equivalent geometric imperfections. In general, a very good agreement can be observed, and buckling modes obtained from FEA are almost the same as those from measurement, both are interactive buckling of multiple folds. For test specimens W1 and W3, the buckling range is relatively small, which is concentrated at the middle of web height. However, the buckling range is extended to the entire web height or the area between bottom flange and horizontal stiffeners after the installation of vertical stiffeners for test specimens W2 and W4.

3.2. Load-deflection curves

Under a concentrated load P at mid-span section, the deflection (Δ) at mid-span of the simply supported steel I-girder with corrugated steel web can be calculated as $\Delta = P/k_0$, in which k_0 is the initial stiffness at elastic stage, which can be obtained considering bending stiffness k_b and shear stiffness k_s simultaneously:

$$k_0 = \frac{k_b k_s}{k_b + k_s} \tag{2}$$

$$k_b = \frac{48EI}{L^3} \tag{3}$$

$$k_s = \frac{4A_w G}{L}\eta \tag{4}$$

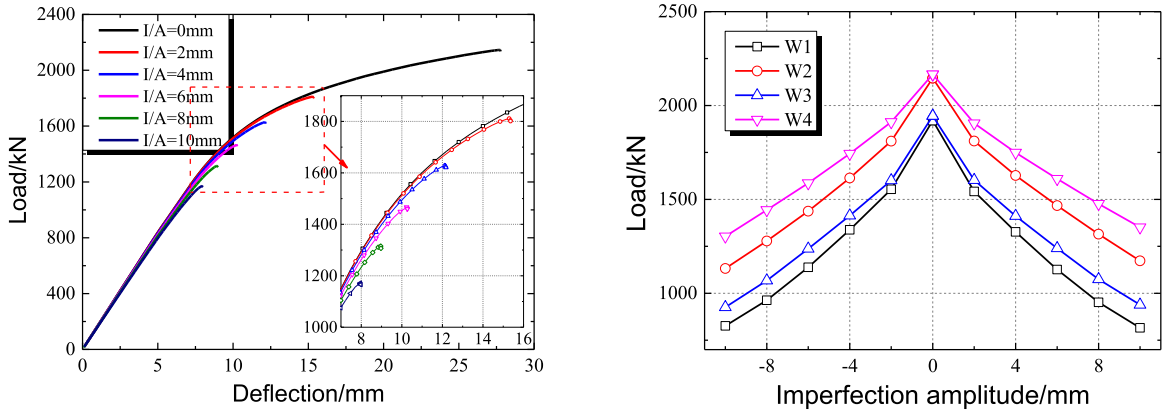

(a) Load-deformation curves for specimen W2 (b) Relationship between loading capacity andI/A

Fig. 11. Effect of equivalent imperfection amplitude.

(a) Experimental bucking mode of W1

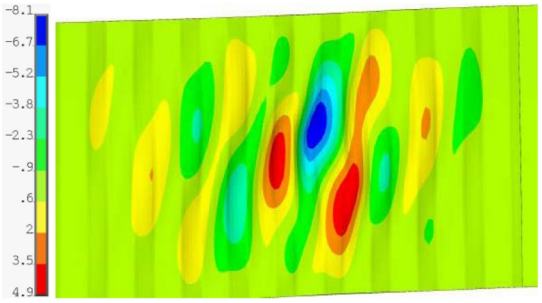

(b) FEA bucking mode of W1(mm)

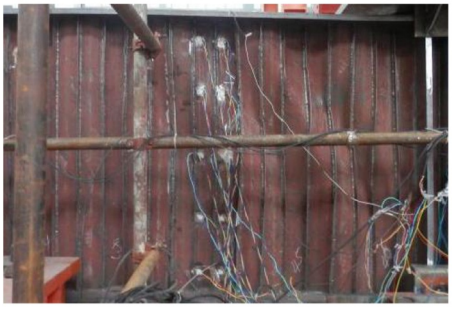

(c) Experimental bucking mode of W2

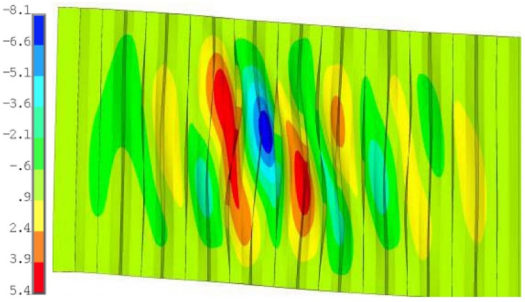

(d) FEA bucking mode of W2 (mm)

(e) Experimental bucking mode of W3

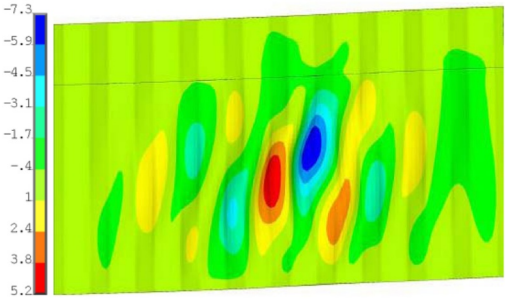

(f) FEA bucking mode of W3 (mm)

(g) Experimental bucking mode of W4

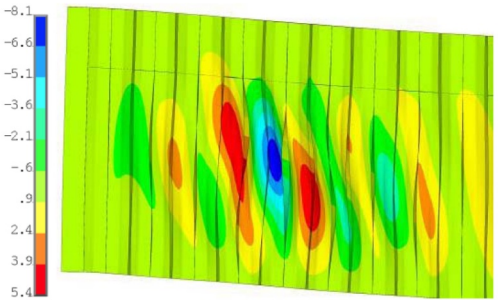

(h) FEA bucking mode of W4 (mm)

Fig. 12. Comparison of failure modes obtained from test and FEA.

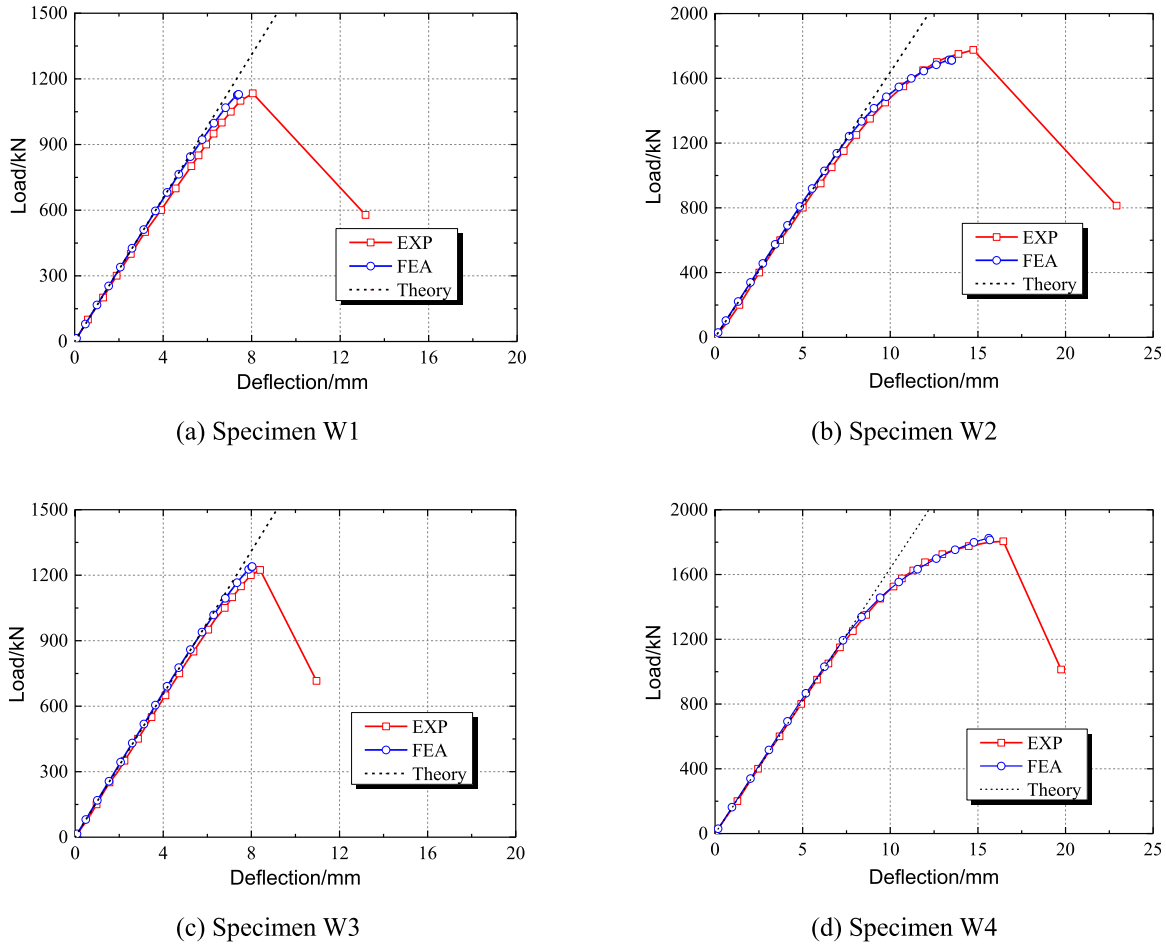

Fig. 13. Load-displacement curves obtained from test and FEA.

where, G is the elastic modulus and shear modulus, respectively; I is the moment of inertial of the section, neglecting the web's contribution duo to its according effect, but the contribution of horizontal stiffeners were considered; A_w is the sectional area of corrugated steel web; L is the span of simply supported girder; η is the shape coefficient of corrugated steel web, $\eta = (a+b)/(a+c)$, which reflects the influence of web corrugation.

The relationships of applied load and mid-span deflection for all the specimens were obtained from tests, theory and FEA, as shown in Fig. 13. The load-displacement curves from numerical studies agree well with those from measured and calculated results in terms of both stiffness and strength. The predicted load-displacement curves from FE models do not show a descending branch, because force control method was adopted in FE models, and the calculation is difficult to converge after web buckling. In the elastic stage, the load-displacement curves from the theoretical calculation, finite element simulation, and model tests are coincident with each other. For specimens W2 and W4, since shear yielding of corrugated web first occurred, the load-displacement curve from finite element simulation showed a significant nonlinear segment, and the position of the curve entering into nonlinearity obtained from FEA is coincident with that from the test.

3.3. Shear capacity

The FE model described above was used to predict the shear behavior of steel I-girders with stiffened corrugated steel web. Table 1 shows the comparison of ultimate load P_u and deflection Δ_u between experimental and FEA results, φ_u is improvement coefficient of shear capacity for steel girder with stiffened corrugated web, i.e. the ratio of the shear capacity of specimens with stiffeners to that of specimen W1. The ratios of simulated ultimate load (P_{u_FEA}) to measured one (P_{u_test}) for specimens W1~W4 are 1.00, 0.95, 1.01, and 1.00, respectively, and the average value is 0.99. The ratio of simulated deflection (Δ_{u_FEA}) to measured ones (Δ_{u_test}) are 0.92, 0.91, 0.96, and 0.94, respectively, and the average value is 0.93. The comparison indicates that established FE models can be used to predict the shear behavior including shear strength and stiffness of stiffened corrugated steel web girders.

3.4. Strain distributions of the cross-section

Fig. 14 shows the comparison of tested and simulated normal strain distribution at section A-A under the applied load of 400 kN. The strain distributions from FEA agree well with that from the test. The longitudinal strain of corrugated steel web is relatively small, indicating that corrugated steel web does not resist bending moment, and vertical stiffeners do not affect the longitudinal stiffness of corrugated steel web. There is a sudden change of longitudinal strain at the position near horizontal stiffeners for specimens W3 and W4, indicating that the horizontal stiffeners increase the longitudinal stiffness of corrugated steel web. However, since the thickness of horizontal stiffeners is much smaller than that of steel flanges, the normal strain just changes slightly.

4. Parametric analysis

From the above analysis and validation, it can be found that the finite element models can accurately simulate the shear behavior of stiffened corrugated steel web girders. Subsequently, a series of FE

Table 1
Comparison of ultimate load and deflection between experimental and FEA results.

Specimen	P_{u_test} (kN)	P_{u_FEA} (kN)	φ_{u_test}	φ_{u_FEA}	Δ_{u_test} (mm)	Δ_{u_FEA} (mm)	P_{u_FEA}/P_{u_test}	$\varphi_{u\_FEA}/\varphi_{u\_test}$	$\Delta_{u\_FEA}/\Delta_{u\_test}$
W1	1134	1129	1.00	1.00	8.05	7.41	1.00	1.00	0.92
W2	1775	1714	1.57	1.52	14.74	13.47	0.97	0.97	0.91
W3	1224	1240	1.08	1.10	8.40	8.04	1.01	1.02	0.96
W4	1805	1824	1.59	1.62	16.45	15.62	1.01	1.02	0.95
Average							1.00	1.00	0.94

models were performed to examine the effects of thickness of the corrugated web and stiffeners, the corrugation depth and the height of stiffeners, on the shear behavior of steel girders with stiffened corrugated web.

4.1. Effect of web thickness

The effect of web thickness on shear behavior of stiffened corrugated steel web was investigated by changing the web thickness from 1 mm to 6 mm with an increment of 1 mm. Fig. 15 shows the effects of web thickness on load-deflection curves and loading capacity. Fig. 16 shows the failure modes of specimens W1∼3 with different web thickness, the buckling modes for specimen W4 with hybrid vertical and horizontal stiffeners are similar to that of specimen W2 with vertical stiffeners, but the buckling area of W4 is located below horizontal stiffeners.

The loading capacity almost increases linearly for corrugated web girders with vertical stiffeners as the increase of web thickness. Additionally, increasing the web thickness of stiffened corrugated steel web girder leads to a significant increase of initial stiffness. In order to ensure web yielding before web buckling, the thickness of corrugated steel web with vertical stiffeners must be thicker than 3 mm while the thickness of pure corrugated steel web must be thicker than 5 mm. For specimen W1 with pure corrugated web and specimen W3 with horizontal stiffeners, the failure modes experience local, interactive and global buckling with the increase of web thickness from 1 mm to 6 mm. However, steel girders with vertical stiffeners all exhibit interactive buckling modes. Thus, vertical stiffeners can prevent local buckling of corrugated web with a small thickness and postpone the occurrence of global buckling with the increase of web thickness. For specimen W3 with a web thickness of 6 mm, the horizontal stiffeners deformed with corrugated web, the influence of horizontal stiffeners on buckling mode can be negligible, so the shear capacity of thick (6 mm) corrugated web with or without horizontal stiffeners is almost the same.

4.2. Effect of corrugation depth

The effect of corrugation depth on shear behavior of stiffened corrugated steel web girder was investigated by changing the corrugation depth from 10 mm to 90 mm with an increment of 20 mm. The

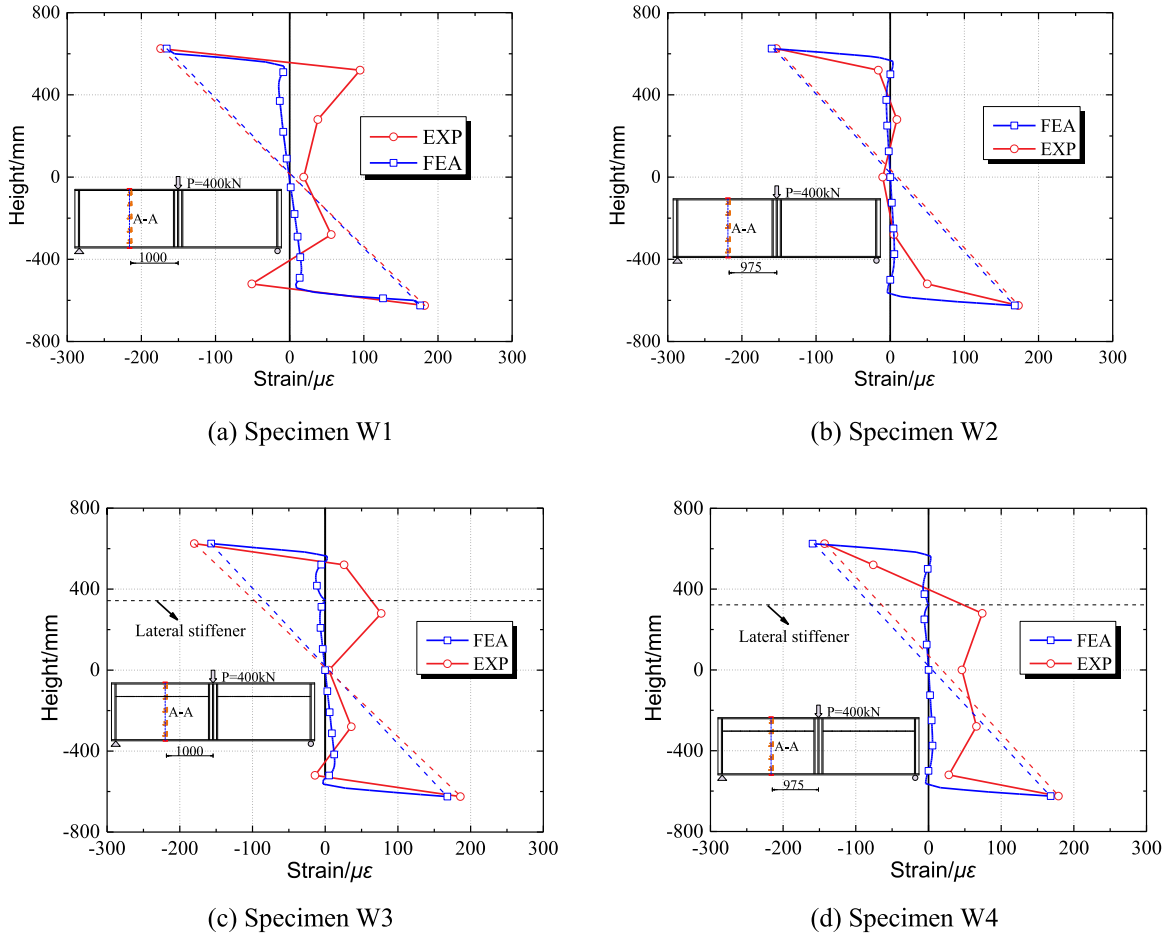

(a) Specimen W1

(b) Specimen W2

(c) Specimen W3

(d) Specimen W4

Fig. 14. Normal strains obtained from test and FEA.

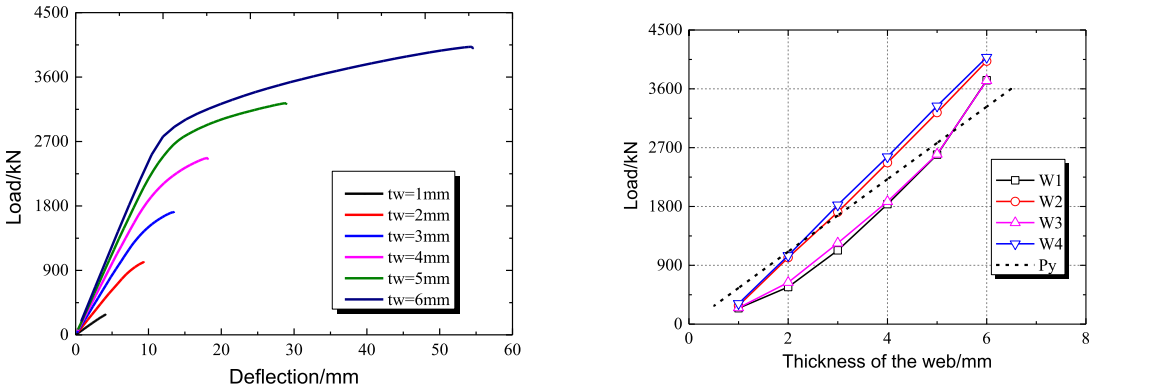

(a) Load-deflection curves of specimen W2 (b) Relationship between loading capacity and web thickness

Fig. 15. Effects of web thickness on load-deflection curves and loading capacity.

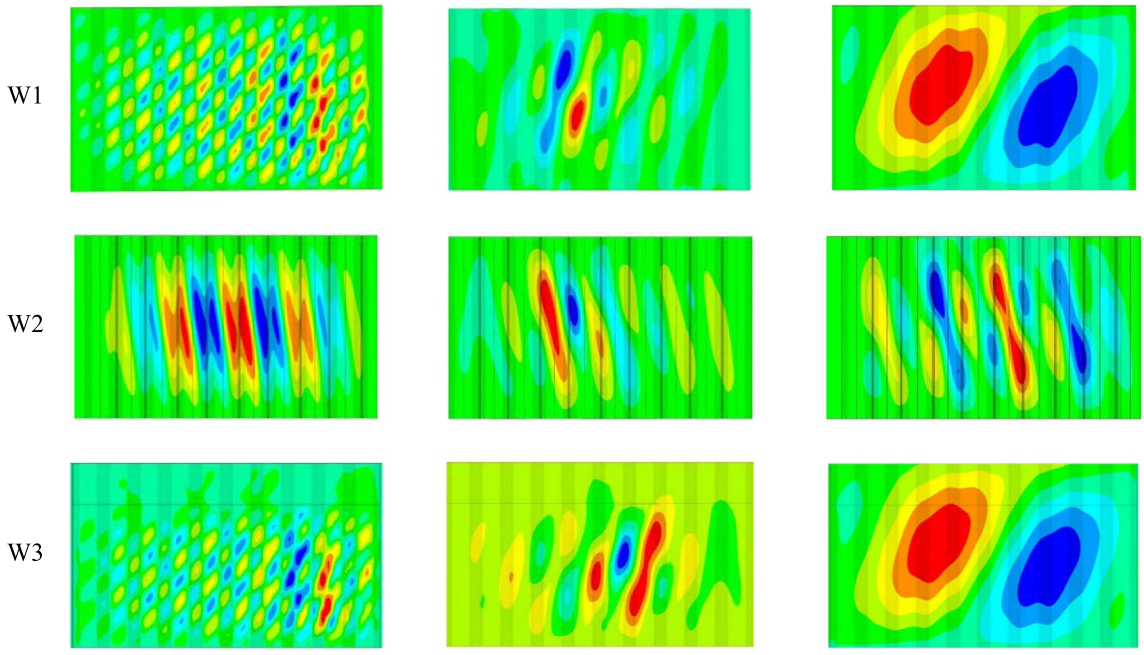

(a) t_w=1mm (b) t_w=4mm (c) t_w=6mm

Fig. 16. Effect of the web thickness on failure mode.

corrugation angle α (Fig. 2) is calculated as 6°, 18°, 29°, 38°, and 45° when corrugation depth changes from 10 mm to 90 mm, in order to keep the width of sub-panel unchanged. Fig. 17 shows the effects of corrugation depth on load-deflection curves and loading capacity of stiffened corrugated web girders. Fig. 18 shows the failure modes of specimens W1~3 with different corrugation depth.

It can be noticed that increasing the corrugation depth slightly decreases the initial stiffness. For vertical stiffened corrugated web girders, the shear strength increases almost linearly with the increase of corrugation depth (less than 50 mm), while the increment becomes smaller in cases of large corrugation depth (more than 50 mm). Corrugated steel web girders with small corrugation depth (10 mm) are failed by global bucking, while those with relatively large corrugation depths exhibit interactive or local buckling. For specimens W1 and W3, the shear strength is reduced when the buckling mode changes from interactive buckling to local buckling, because the shear strength is more sensitive to the local buckling imperfection shape introduced into finite element model compared with interactive buckling with the same imperfection amplitude. For specimens W1 and W2 with a corrugation depth of 90 mm, the failure modes are local and interactive buckling, respectively; the vertical stiffeners can delay the occurrence of local buckling with the increase of corrugation depth. However, elastic local buckling occurs for specimen W3 with a corrugation depth of 70 mm; while specimen W1 shows interactive buckling, the horizontal stiffeners advanced the occurrence of local buckling.

4.3. Effect of stiffeners thickness

The effect of stiffeners thickness on shear behavior of stiffened corrugated steel web girder was investigated by changing the thickness of stiffeners (t_s) for specimens W2~W4. The thickness ranges from 0 mm to 9 mm with an increment of 2 mm. Fig. 19 shows the effects of stiffeners' thickness on load-deflection curves and loading capacity. It can be concluded that the loading capacity increases with the increase of vertical stiffeners' thickness, but the initial stiffness is not changed. Increasing the thickness of horizontal stiffeners leads to a slight increase of the initial stiffness, because the horizontal stiffener increases the bending stiffness of corrugated steel web girder, but the cross-section area of the horizontal stiffener is smaller than that of the top and bottom flanges, resulting in small increasing amplitude. For specimen

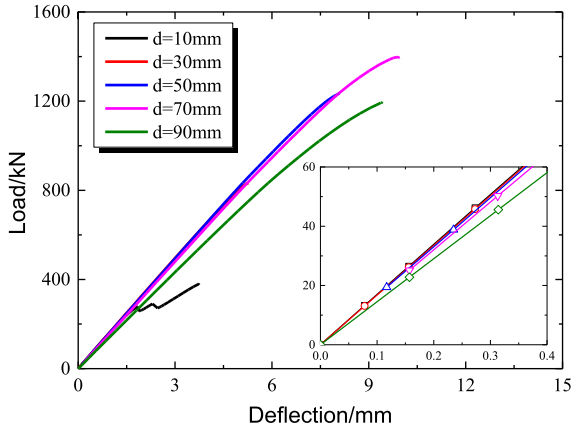

(a) Load-deformation curves of specimen W1

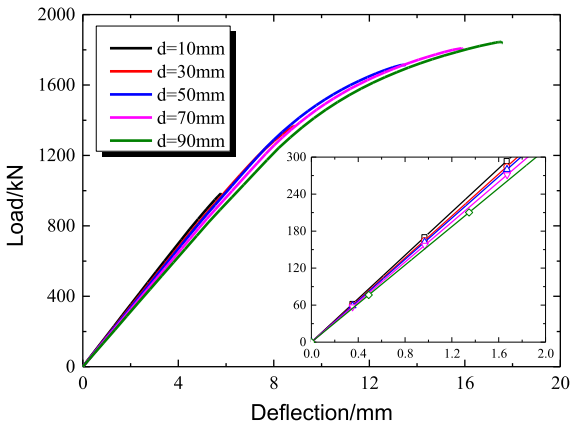

(b) Load-deformation curves of specimen W2

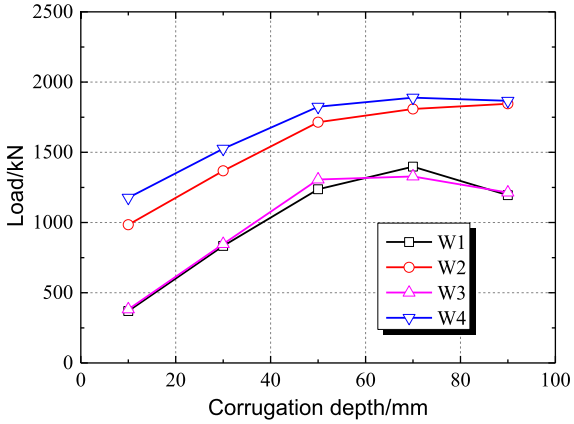

(c) Relationship between loading capacity and corrugation depth

Fig. 17. Effects of corrugation depth on load-deflection curves and loading capacity.

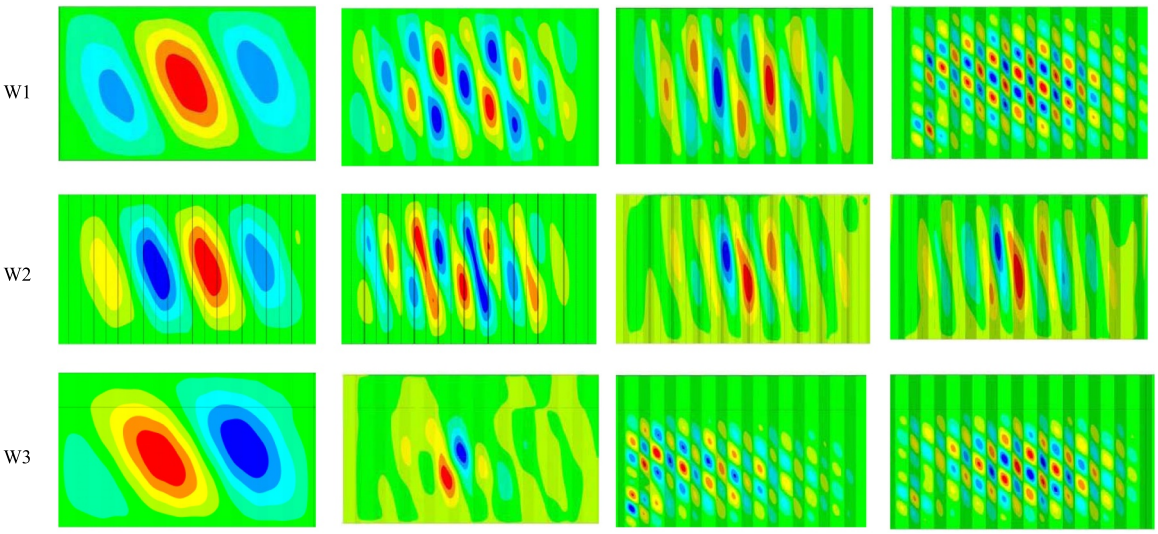

(a) *d*=10mm (c) *d*=30mm (c) *d*=70mm (c) *d*=90mm

Fig. 18. Effect of corrugation depth on failure mode.

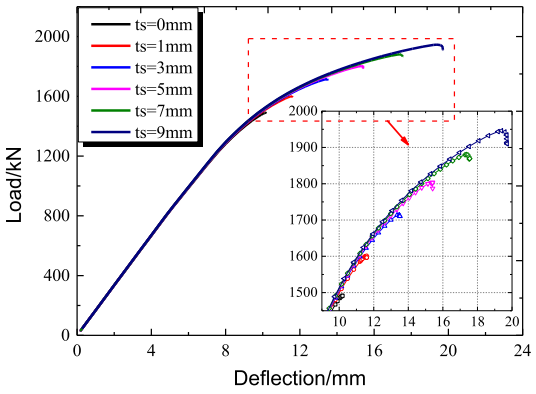

(a) Load-deflection curves for specimen W2

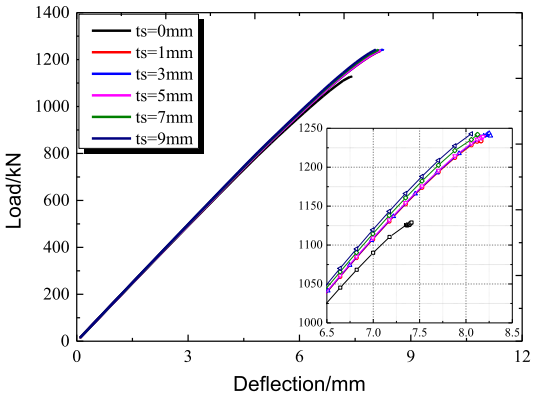

(b) Load-deflection curves for specimen W3

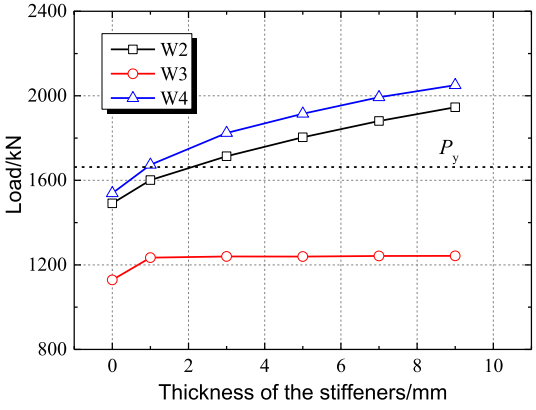

(c) Relationship between loading capacity and stiffener thickness

Fig. 19. Effect of stiffener thickness on load-deflection curves and loading capacity.

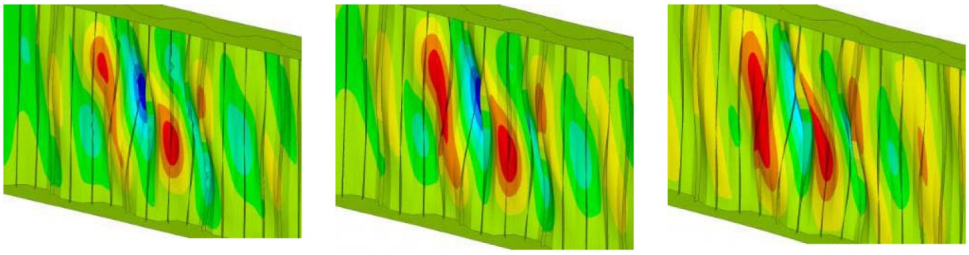

(a) t_s=1mm (b) t_s=3mm (c) t_s=9mm

Fig. 20. Effect of stiffener thickness on failure mode.

with vertical stiffeners, the thickness of the stiffeners should be greater than 3 mm to guarantee the nonlinear buckling failure. For specimen with horizontal stiffeners, the increase of horizontal stiffeners' thickness does not affect the shear capacity, since shear buckling occurs at corrugated steel webs below horizontal stiffeners. Fig. 20 shows the influence of stiffeners' thickness on the failure modes of specimen W2. The vertical stiffeners deformed with the buckling of corrugated web. When the thickness of stiffener is small (1 mm), elastic local bucking firstly appeared on the stiffeners, the benefit of stiffeners is not fully developed. With the increase of stiffeners' thickness, the stiffeners' restraining effect on the web is enhanced and the bucking area along the web height is enlarged.

4.4. Effect of stiffeners height

The effect of stiffeners' height on shear behavior of stiffened corrugated steel web was investigated by changing the height of stiffeners (h_s) for specimens W2~W4. The stiffeners' height ranges from 0 mm to 45 mm with an increment of 10 mm. Fig. 21 shows the influence of stiffeners height on load-deflection curves and loading capacity. It can be seen that the height of vertical stiffeners does not affect the initial stiffness, but the loading capacity increases with the increase of stiffeners height. In order to ensure nonlinear buckling failure of test specimens, the stiffeners' height should be greater than 25 mm. Increasing the height of horizontal stiffeners leads to slight increase of the initial stiffness and loading capacity. When the horizontal stiffeners'

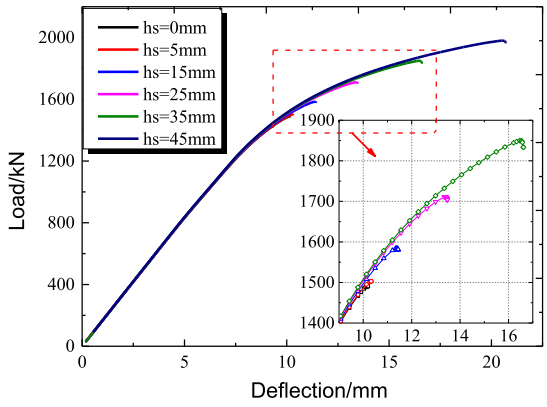

(a) Load-deformation curves for specimen W2

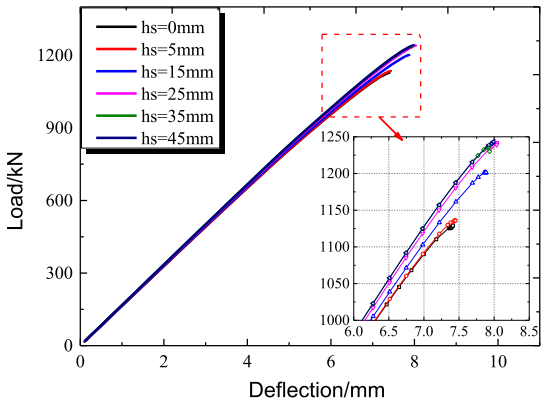

(b) Load-deformation curves for specimen W3

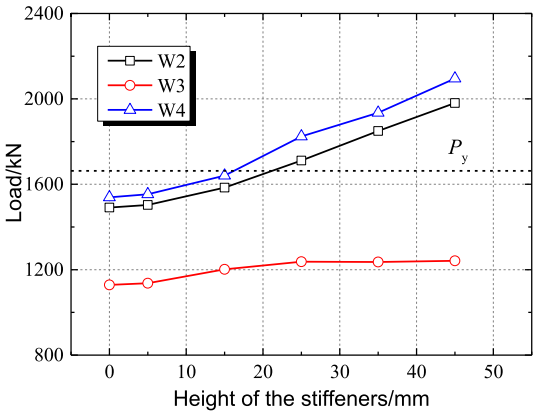

(c) Relationship between loading capacity and stiffener height

Fig. 21. Effect of stiffener height on load-deflection curves and loading capacity.

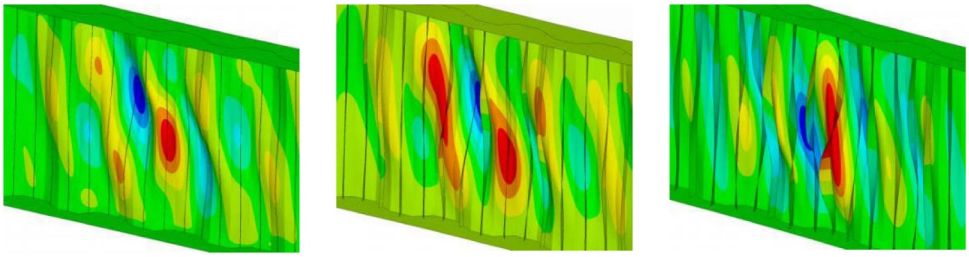

(a) h_s=5mm (b) h_s=25mm (c) h_s=45mm

Fig. 22. Effect of stiffener height on failure mode.

height is more than 25 mm, it has negligible influence on shear strength and failure mode, since the stiffeners' stiffness is sufficient to ensure the buckling occurs below the horizontal stiffeners. Fig. 22 shows the influence of stiffeners' height on the failure mode of specimen W2. When the height of vertical stiffeners is small (5 mm), the buckling area is concentrated at the center of web height, which is similar to that of pure corrugated web beam. With the increase of the vertical stiffeners' height, buckling area is extended to the whole web height.

5. Evaluation of shear strength

Shear strength of steel I-girder is controlled by buckling and/or shear yielding of corrugated steel web. Shear buckling of corrugated webs is often classified as local buckling, global buckling, and interactive buckling. Global buckling involves multiple folds and the buckled shape extends diagonally over the height of the web. Local buckling is controlled by deformations within a single "fold" of the web. The interactive shear buckling mode is attributed to the interaction between local and global shear buckling modes.

5.1. Local shear buckling

The local elastic shear buckling stress of a corrugated steel web can be predicted using classic plate buckling theory [43]. A single parallel

or inclined fold is assumed to be supported by the adjacent folds and steel flanges. The corresponding local elastic shear buckling stress, $\tau^e_{cr,L}$ is:

$$\tau^e_{cr,L} = k_L \frac{\pi^2 E}{12(1-\upsilon^2)}\left(\frac{t_w}{w}\right)^2 \tag{5}$$

where w is the maximum fold width, which is the larger value of a and c; k_L is the local shear buckling coefficient that depends on the boundary conditions and the fold aspect ratio, k_L lies between 5.34 (assuming simply supported edges) and 8.98 (assuming fixed edges). $k_L = 5.34$ is recommend for practical design purposes by Moon et al. [44].

5.2. Global shear buckling

An expression for the global elastic shear buckling stress of a corrugated steel plate, $\tau^e_{cr,G}$ was developed by Easley et al. [10] using orthotropic plate theory:

$$\tau^e_{cr,G} = k_G \frac{D_x^{3/4} D_y^{1/4}}{t_w h_w^2} \tag{6}$$

where, k_G is global shear buckling coefficient, D_x and D_y are the bending stiffness per unit length of corrugated web associated with x- and y-axes; Easley et al. [11] proposed that k_G varies between 36 (assuming the web is simply supported by the flanges) and 68.4 (assuming that the flanges provide the web with fixed supports). However, Elgaaly [45] suggested that k_G should be taken as 31.6 for simply supported boundaries and 59.2 for clamped boundaries. D_x and D_y for trapezoidal corrugated webs are determined as follows:

$$D_x = \frac{EI_x}{a+b} \tag{7}$$

$$D_y = \frac{Et_w^3}{12}\frac{a+b}{a+c} \tag{8}$$

where, I_x is the moment of inertia about the x-axis, $I_x = 2at_w(d/2)^2 + d^3t_w/(6\sin\alpha)$.

According to the design manual for PC bridges with corrugated steel webs [46], D_x and D_y can be calculated as:

$$D_x = \frac{Et_w^3[(d/t_w)^2+1]}{6\eta} \tag{9}$$

$$D_y = \frac{Et_w^3}{12(1-\upsilon^2)}\eta \tag{10}$$

where, η is the length reduction factor defined as $\eta = (a+b)/(a+c)$.

Abbas [47] expressed the global shear buckling stress directly in terms of geometric parameters of the trapezoidal corrugations (Fig. 2) as follows:

$$\tau^e_{cr,G} = k_G \frac{Et_w^{1/2}a^{3/2}}{12h_w^2} F(\alpha,\beta) \tag{11}$$

where, $F(\alpha, \beta)$ is a coefficient based on the web corrugation geometry, as follows:

$$F(\alpha,\beta) = \sqrt{\frac{(1+\beta)\sin^3\alpha}{\beta+\cos\alpha}}\cdot\left\{\frac{3\beta+1}{\beta^2(\beta+1)}\right\}^{3/4} \tag{12}$$

where, β is the ratio of a to c, generally $\beta = 1.0$.

5.3. Interactive shear buckling

The interactive shear buckling mode is attributed to the interaction between local and global shear buckling modes and governs shear buckling strength. Lindner & Aschinger [48] first provided interactive elastic shear buckling stress, $\tau^e_{cr,I}$, as follows:

$$\tau^e_{cr,I} = \frac{\tau^e_{cr,L}\cdot\tau^e_{cr,G}}{((\tau^e_{cr,G})^n + (\tau^e_{cr,L})^n)^{1/n}} \tag{13}$$

where, the exponent n is an integer, different researchers have given a different value of n [2,3,14,16,38,49].

5.4. Shear strength

Previous studies [14,44] have shown that shear strength of corrugated steel web was generally controlled by interactive shear buckling strength, so the shear buckling coefficient ($\lambda_{I,n}$) of corrugated steel web is defined as:

$$\lambda_{I,n} = \sqrt{\tau_y/\tau^e_{cr,I}} \tag{14}$$

where, τ_y is shear yield stress of corrugated steel web.

Driver et al. [38] proposed Eq. (15) to calculate the shear capacity of corrugated steel webs, it was recommended that n equals to 2 in Eq. (13), this equation covers all shear failure modes, including inelastic buckling and shear yielding:

$$\tau_{n,D} = \sqrt{\frac{(\tau^e_{cr,L}\cdot\tau^e_{cr,G})^2}{(\tau^e_{cr,G})^2 + (\tau^e_{cr,L})^2}} \tag{15}$$

When the elastic shear buckling stress ($\tau^e_{cr,G}$, $\tau^e_{cr,L}$) exceeds 80% of shear yield stress τ_y, the inelastic shear buckling stress τ^{in}_{cr} should be considered as following [45]:

$$\tau^{in}_{cr} = \sqrt{0.8\tau_y\tau^e_{cr}} \le \tau_y \tag{16}$$

Moon et al. [44] proposed Eq. (17) to calculate the shear capacity of corrugated steel webs. It was suggested that n equals to 1 in Eq. (13), the equation considers the reduction of shear strength due to material nonlinearity, residual stress, and initial imperfection [46]:

$$\tau_{n,Moon} = \tau_y \times \begin{cases} 1 & \lambda_{I,1} < 0.6 \\ 1 - 0.614(\lambda_{I,1} - 0.6) & 0.6 \le \lambda_{I,1} \le \sqrt{2} \\ 1/\lambda^2_{I,1} & \sqrt{2} < \lambda_{I,1} \end{cases} \tag{17}$$

El-Metwally [49] proposed Eq. (18) to calculate the shear capacity of corrugated steel web, which includes shear yield stress, and the interactive shear buckling coefficient is taken as $n = 2$:

$$\tau_{n,EL} = \tau_y \times (1/((\lambda_{I,2})^4 + 1))^{1/2} \tag{18}$$

Sauce and Braxtan [16] summarized a large number of previous experimental data, and selected 22 groups of experimental results to fit Eq. (19) to calculate the shear capacity of corrugated steel web, and the interactive shear buckling coefficient is taken as $n = 3$:

$$\tau_{n,Sauce} = \tau_y \times (1/((\lambda_{I,3})^6 + 2))^{1/3} \tag{19}$$

Hassanein and Kharoob [2] believed that the boundary conditions between corrugated steel web and top/bottom flanges are close to fixed conditions, and proposed Eq. (20) to calculate shear capacity under such boundary conditions, in which the interactive shear buckling coefficient is taken as $n = 0.6$, the local buckling (k_L) and the global buckling (k_G) coefficients are taken as the upper limit of 8.98 and 59.2, respectively

$$\tau_{n,Hassanein} = \tau_y \times (1/((\lambda_{I,0.6})^6 + 2))^{1/3} \tag{20}$$

Leblouba et al. [3] recently collected 113 test results from literature and carried out 12 tests by themselves, and developed an analytical model to calculate shear strength of corrugated steel web based on the hyperbolic Richards equation, which is given as follows:

$$\tau_{n,\text{Leblouba}} = \tau_y \times (1/((\lambda_{I,4}/1.58)^{1.6} + 1))^{1.15} \tag{21}$$

The applicability of these above calculation methods on shear capacity to stiffened corrugated steel web was evaluated based on experimental and numerical results. Table 2 summarizes the analytical

Table 2
Comparison of calculated shear strength with test results.

Specimens	Test (kN)	Calculation (kN)						Ratio					
	P_{u_test}	$P_{u,M}$	$P_{u,D}$	$P_{u,S}$	$P_{u,E}$	$P_{u,H}$	$P_{u,L}$	$P_{u,M}/P_{u\_test}$	$P_{u,D}/P_{u\_test}$	$P_{u,S}/P_{u\_test}$	$P_{u,E}/P_{u\_test}$	$P_{u,H}/P_{u\_test}$	$P_{u,L}/P_{u\_test}$
W1	1134	1278	1176	1239	1303	1193	1153	1.13	1.04	1.09	1.15	1.05	1.02
W2	1775	1306	1176	1255	1338	1208	1176	0.74	0.66	0.71	0.75	0.68	0.66
W3	1224	1421	1176	1295	1464	1260	1274	1.16	0.96	1.06	1.20	1.03	1.04
W4	1805	1441	1176	1299	1481	1267	1290	0.80	0.65	0.72	0.82	0.70	0.71

shear strength of specimens W1~W4, and compares calculated results with test ones. For specimens W3 and W4, since the buckling of corrugated steel web occurred between horizontal stiffeners and bottom flange, the effective height of the web h_w is taken as the distance from horizontal stiffeners to bottom flange (h_w = 930 mm) when global elastic buckling stress $\tau^e_{cr,G}$ of stiffened corrugated steel web is calculated. For specimens W2 and W4, corrugated steel web girder with vertical stiffeners, the contribution of vertical stiffeners to the moment of inertia is considered when calculating the shear capacity of stiffened corrugated steel web girders.

As summarized in Table 2, for specimens W1 and W3 without vertical stiffeners, the calculation methods proposed by Moon et al. [44] and El-Metwally [49] seriously overestimate their shear capacity, with an average error of 14% and 17% respectively. Sauce & Braxtan [16] method also overestimates the shear capacity, with an average error of 8%. The method proposed by Driver et al. [38] slightly overestimates the shear strength for specimen W1 but underestimates specimen W3. The calculation methods suggested by Hassanein & Kharoob [2] and Leblouba et al. [3] predict shear strength of corrugated steel web much better, with an average error of 4% and 3%, respectively. For corrugated steel web girders with vertical stiffeners (specimens W2 and W4), the above-mentioned calculation methods seriously underestimate their shear strength. The relative errors are 18~35% with the average value of 28%.

Fig. 23 shows the comparison of different calculation methods to numerical and test results. Most of the numerical data based on specimen W1 and W3 are below the buckling curves proposed by Moon et al. [44] and El-Metwally [49]. The curves according to Driver et al. [38] and Sauce & Braxtan [16] passed through the numerical data for specimens without vertical stiffeners. Curves according to Hassanein & Kharoob [2] and Leblouba et al.[3] agree well with the numerical data, except for some cases with very small web thickness. Nevertheless, all of these curves are below the numerical data of specimens with vertical stiffeners. Therefore, calculation methods presented by Hassanein & Kharoob [2] and Leblouba et al. [3] can be used to predict shear strength of corrugated web without stiffeners more accurately. All of these above methods are not applicable to the corrugated steel web with vertical stiffeners. The calculation method to accurately predict shear capacity of stiffened corrugated steel web will be developed and described in further study.

6. Conclusions

The current paper explores the shear performance of stiffened corrugated steel web girders numerically and analytically. The following conclusions can be drawn from the present study:

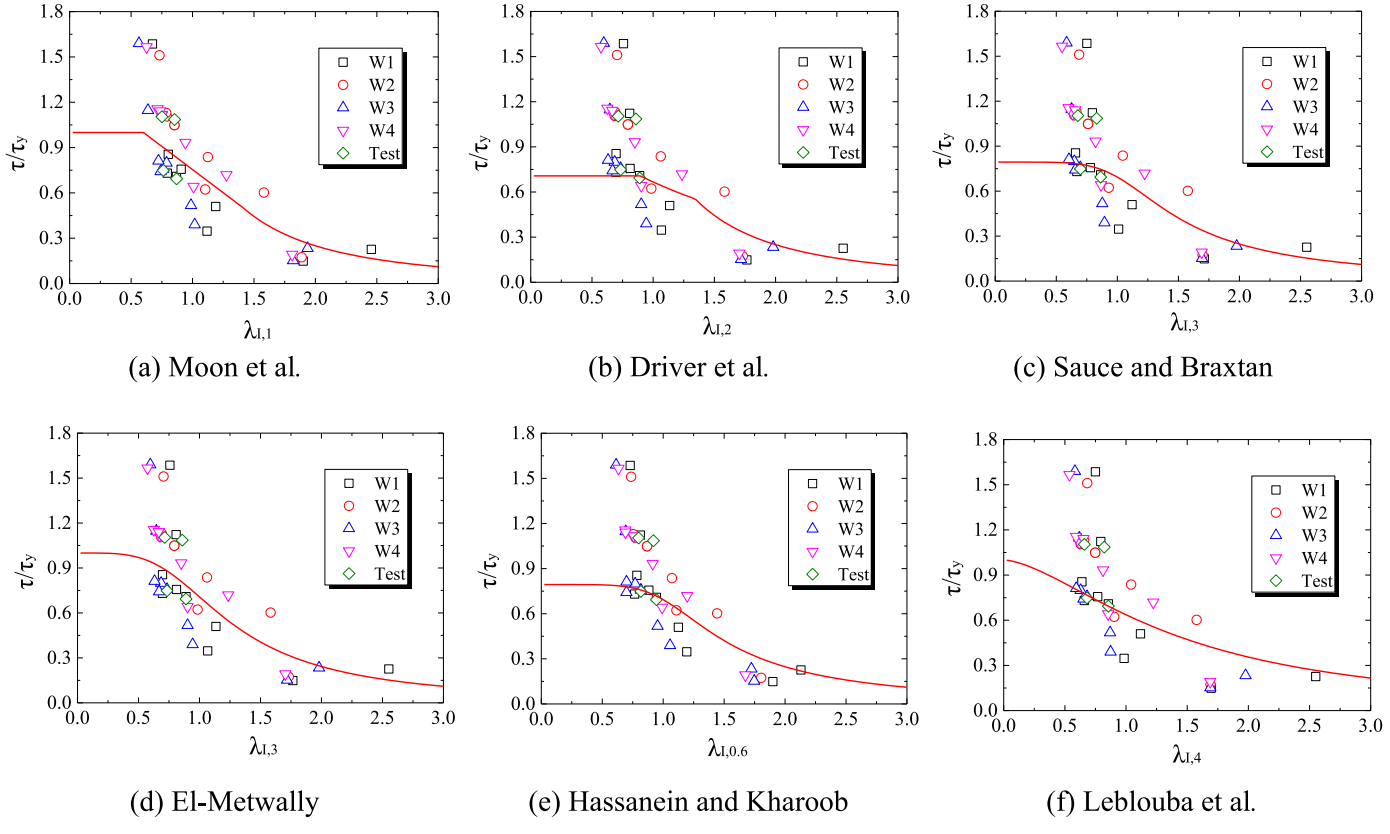

Fig. 23. Calculated shear strength compared with numerical and test results.

(1) The established finite element models considering material nonlinearity, welding residual stress and geometric imperfections were validated by experimental results, which can be used to simulate shear behaviors of stiffened corrugated steel web girders.
(2) The shear strength of stiffened corrugated steel web decreased linearly with the increase of the equivalent imperfection amplitude. The sensitivity of corrugated steel webs to geometric imperfections decreased after installation stiffeners, especially for the combination of vertical and lateral stiffeners. The welding residual stress will cause the webs to enter the nonlinearity in advance and reduce the loading capacity of stiffened corrugated steel web girders.
(3) With the increase of the corrugation depth (corrugation angle), the buckling modes experience global, interactive and local buckling for pure corrugated web. The vertical stiffeners can postpone the occurrence of local buckling while the horizontal stiffeners cause the occurrence of local buckling in advance.
(4) The shear strength of stiffened corrugated steel web increased with the increase of the thickness and height of vertical stiffeners. For corrugated steel web with a thickness of 3 mm and corrugation depth of 50 mm, the thickness and height of vertical stiffeners should be greater than 3 mm and 25 mm to guarantee nonlinear buckling failure.
(5) The calculation methods proposed by Hassanein & Kharoob [2] and Leblouba et al. [3] can be used to predict shear strength of corrugated steel web more accurately. All of existing methods underestimate the shear strength of vertical stiffened corrugated steel web. A calculation method to accurately predict shear capacity of stiffened corrugated steel web needs to be developed in further study.

Acknowledgments

The authors gratefully thank the financial support of National Natural Science Foundation of China (51308070) and Transportation Science and Technology Project of Sichuan Province (110109039).

References

[1] S. Wang, J. He, Y. Liu, Shear behavior of steel I-girder with stiffened corrugated webs, Part I: Exp. Study (2019) (Submitted publication).
[2] M.F. Hassanein, O.F. Kharoob, Behavior of bridge girders with corrugated webs: (i) Real boundary condition at the juncture of the web and flanges, Eng. Struct. 57 (2013) 554–564, https://doi.org/10.1016/j.engstruct.2013.03.004.
[3] M. Leblouba, S. Barakat, S. Altoubat, T.M. Junaid, M. Maalej, Normalized shear strength of trapezoidal corrugated steel webs, J. Constr. Steel Res. 136 (2017) 75–90, https://doi.org/10.1016/j.jcsr.2017.05.007.
[4] J. He, Y. Liu, A. Chen, T. Yoda, Mechanical behavior and analysis of composite bridges with corrugated steel webs: state-of-the-art, Int. J. Steel Struct. 12 (2012) 321–338, https://doi.org/10.1007/s13296-012-3003-9.
[5] R.J. Jiang, F. Tat, K. Au, Y.F. Xiao, Prestressed Concrete Girder Bridges with Corrugated Steel Webs: review, J. Struct. Eng. Asce. 141 (2015) 1–9, https://doi.org/10.1061/(ASCE)ST.1943-541X.0001040.
[6] J. He, Y. Liu, A. Chen, D. Wang, T. Yoda, Bending behavior of concrete-encased composite I-girder with corrugated steel web, Thin-Walled Struct. 74 (2014) 70–84, https://doi.org/10.1016/j.tws.2013.08.003.
[7] J. He, Y. Liu, Z. Lin, A. Chen, T. Yoda, Shear behavior of partially encased composite I-girder with corrugated steel web: numerical study, J. Constr. Steel Res. 79 (2012) 166–182, https://doi.org/10.1016/j.jcsr.2012.07.018.
[8] J. He, Y. Liu, Z. Lyu, C. Li, Effects of encased concrete on mechanical behaviors of composite girder bridge with corrugated steel webs, Bridg. Constr. 47 (2017) 54–59.
[9] L. Huang, H. Hikosaka, K. Komine, Simulation of accordion effect in corrugated steel web with concrete flanges, Comput. Struct. 82 (2004) 2061–2069, https://doi.org/10.1016/j.compstruc.2003.07.010.
[10] J.T. Easley, D.E. McFarland, Buckling of light-gage corrugated metal shear diaphragms, J. Struct. Div. Asce. 95 (1969) 1497–1516.
[11] J.T. Easley, Buckling formulas for corrugated metal shear diaphragms, J. Struct. Div. Asce. 101 (1975) 1403–1417.
[12] M. Elgaaly, R.W. Hamilton, A. Seshadri, Shear strength of beams with corrugated webs, J. Struct. Eng. 122 (1996) 390–398, https://doi.org/10.1061/(ASCE).
[13] R. Luo, B. Edlund, Shear capacity of plate girders with trapezoidally corrugated webs, Thin-Walled Struct. 26 (1996) 19–44, https://doi.org/10.1016/0263-8231(96)00006-7.
[14] J. Yi, H. Gil, K. Youm, H. Lee, Interactive shear buckling behavior of trapezoidally corrugated steel webs, Eng. Struct. 30 (2008) 1659–1666, https://doi.org/10.1016/j.engstruct.2007.11.009.
[15] M.E.A.H. Eldib, Shear buckling strength and design of curved corrugated steel webs for bridges, J. Constr. Steel Res. 65 (2009) 2129–2139, https://doi.org/10.1016/j.jcsr.2009.07.002.
[16] R. Sause, T.N. Braxtan, Shear strength of trapezoidal corrugated steel webs, J. Constr. Steel Res. 85 (2013) 105–115, https://doi.org/10.1016/j.jcsr.2013.02.012.
[17] M.F. Hassanein, O.F. Kharoob, Behavior of bridge girders with corrugated webs: (ii) Shear strength and design, Eng. Struct. 57 (2013) 544–553, https://doi.org/10.1016/j.engstruct.2013.04.015.
[18] M. Leblouba, M.T. Junaid, S. Barakat, S. Altoubat, M. Maalej, Shear buckling and stress distribution in trapezoidal web corrugated steel beams, Thin-Walled Struct. 113 (2017) 13–26, https://doi.org/10.1016/j.tws.2017.01.002.
[19] M.F. Hassanein, A.A. Elkawas, A.M. El Hadidy, M. Elchalakani, Shear analysis and design of high-strength steel corrugated web girders for bridge design, Eng. Struct. 146 (2017) 18–33, https://doi.org/10.1016/j.engstruct.2017.05.035.
[20] A. Chajes, S. Britvec, G. Winter, Effects of cold-straining on structural sheet steels, J. Struct. Div. 89 (1963) 1–32.
[21] N. Abdel-Rahman, K.S. Sivakumaran, Material properties models for analysis of cold-formed steel members, J. Struct. Eng. 123 (1997) 1135–1143, https://doi.org/10.1061/(ASCE)0733-9445(1997)123:9(1135).
[22] K.W. Karren, Corner properties of cold-formed steel shapes.pdf, J. Struct. Div. 92 (1967) 401–432.
[23] B. Jáger, L. Dunai, B. Kövesdi, Flange buckling behavior of girders with corrugated web Part II: numerical study and design method development, Thin-Walled Struct. 118 (2017) 238–252, https://doi.org/10.1016/j.tws.2017.05.020.
[24] A.A. Elkawas, M.F. Hassanein, M.H. El-Boghdadi, Numerical investigation on the non-linear shear behaviour of high-strength steel tapered corrugated web bridge girders, Eng. Struct. 134 (2017) 358–375, https://doi.org/10.1016/j.engstruct.2016.12.044.
[25] R. Luo, B. Edlund, Ultimate strength of girders with trapezoidally corrugated webs under patch loading, Thin-Walled Struct. 24 (1996) 135–156.
[26] C.C. Weng, T. Pekoz, Residual stresses in cold-formed steel members, J. Struct. Eng. Asce. 116 (1990) 1611–1625.
[27] S.H. Lho, C.H. Lee, J.T. Oh, Y.K. Ju, S.D. Kim, Flexural capacity of plate girders with very slender corrugated webs, Int. J. Steel Struct. 14 (2014) 731–744, https://doi.org/10.1007/s13296-014-1205-z.
[28] G.Q. Li, J. Jiang, Q. Zhu, Local buckling of compression flanges of H-beams with corrugated webs, J. Constr. Steel Res. 112 (2015) 69–79, https://doi.org/10.1016/j.jcsr.2015.04.014.
[29] B. Jáger, L. Dunai, B. Kövesdi, Flange buckling behavior of girders with corrugated web Part I: experimental study, Thin-Walled Struct. 118 (2017) 181–195, https://doi.org/10.1016/j.tws.2017.05.021.
[30] T. Sumiya, K. Aoki, M. Tomimoto, M. Kano, Shear strength evaluation of corrugated steel web, Prestress. Concr. 43 (2001) 96–101 (in Japanese).
[31] W. Koichi, K. Masahiro, In-plane bending capacity of steel girders with corrugated web plates, J. Struct. Eng. Jsce. 62 (2006) 323–336 (in Japanese).
[32] L. Gannon, Y. Liu, N. Pegg, M.J. Smith, Effect of welding-induced residual stress and distortion on ship hull girder ultimate strength, Mar. Struct. 28 (2012) 25–49, https://doi.org/10.1016/j.marstruc.2012.03.004.
[33] D. Faulkner, Review of effective plating for use in the analysis of stiffened plating in bending and compression, J. Sh. Res. 19 (1975) 1–17.
[34] R. Connor, J. Fisher, W. Gatti, V. Gopalaratnam, B. Kozy, B. Leshki, D.L. McQuaid, R. Medlock, D. Mertz, T. Murphy, D. Paterson, O. Sorensen, J. Yadlosky, Manual for Design, Construction, and Maintenance of Orthotropic Steel Deck Bridges, 2012.
[35] Q. Zhao, Z. Guo, X. Shen, B. Briseghella, Test study on residual stress distribution of hybrid steel u-rib stiffened plates, J. Constr. Steel Res. 121 (2016) 261–267, https://doi.org/10.1016/j.jcsr.2016.01.024.
[36] H. Xin, Y. Liu, J. He, Y. Zhang, Experimental and analytical study on stiffened steel segment of hybrid structure, J. Constr. Steel Res. 100 (2014) 237–258, https://doi.org/10.1016/j.jcsr.2014.04.002.
[37] H.H. Abbas, R. Sause, R.G. Driver, Shear strength and stability of high performance steel corrugated web girders, in: Proceedings, Structural Stability Research Council Annual Technical Session, 2002, (p. 361_87).
[38] R.G. Driver, H.H. Abbas, R. Sause, Shear Behavior of Corrugated Web Bridge Girders, J. Struct. Eng. 132 (2006) 195–203, https://doi.org/10.1061/(ASCE)0733-9445(2006)132:2(195).
[39] EN 1993-1-5, Eurocode 3: Design of steel structures, Part 1-5: Plated structural elements, 2007.
[40] B. Jáger, L. Dunai, B. Kövesdi, Girders with trapezoidally corrugated webs subjected by combination of bending, shear and path loading, Thin-Walled Struct. 96 (2015) 227–239, https://doi.org/10.1016/j.tws.2015.08.015.
[41] J. Yi, H. Gil, K. Youm, H. Lee, Interactive shear buckling behavior of trapezoidally corrugated steel webs, Eng. Struct. 30 (2008) 1659–1666, https://doi.org/10.1016/j.engstruct.2007.11.009.
[42] M. Leblouba, M.T. Junaid, S. Barakat, S. Altoubat, M. Maalej, Shear buckling and stress distribution in trapezoidal web corrugated steel beams, Thin-Walled Struct. 113 (2017) 13–26, https://doi.org/10.1016/j.tws.2017.01.002.
[43] S.P. Timoshenko, J.M. Gere, Theory of Elastic Stability, McGraw-Hill Publishing Co., NewYork, 1961.
[44] J. Moon, J. Yi, B.H. Choi, H.E. Lee, Shear strength and design of trapezoidally corrugated steel webs, J. Constr. Steel Res. 65 (2009) 1198–1205, https://doi.org/10.1016/j.jcsr.2008.07.018.
[45] M. Elgaaly, R.W. Hamilton, A. Seshadri, Shear strength of beams with corrugated webs, J. Struct. Eng. Asce. 122 (1996) 390–398, https://doi.org/10.1061/(ASCE).
[46] Research committee for hybrid structures with corrugated steel web, Design manual for PC bridges with corrugated steel webs (in Japanese), 1998.
[47] H.H. Abbas, Analysis and Design of Corrugated Web I-girders for Bridges Using High Performance Steel, Lehigh University, 2003.
[48] J. Lindner, R. Aschinger, Grenzschubtragfähigkeit von I-trägern mit trapezförmig profilierten Stegen, Stahlbau 57 (1988) 377–380.
[49] A.S. El-Metwally, Prestressed Composite Girders With Corrugated Steel Webs, University of Calgary, 1998.